## James Madison University
# JMU Scholarly Commons

Senior Honors Projects, 2010-current                                    Honors College

Spring 2019

# Investigating the role of integrin beta 3 in dendritic arborization in the supragranular developing cerebral cortex

Zachary Logan Holley
*James Madison University*

Follow this and additional works at: https://commons.lib.jmu.edu/honors201019

 Part of the Developmental Neuroscience Commons, Medical Neurobiology Commons, Molecular and Cellular Neuroscience Commons, Nervous System Commons, Nervous System Diseases Commons, Neurosciences Commons, and the Systems Neuroscience Commons

Investigating the Role of Integrin Beta 3 in Dendritic Arborization in the Supragranular Developing

Cerebral Cortex

_____

An Honors College Project Presented to

the Faculty of the Undergraduate

College of Science and Mathematics

James Madison University

_____

by Zachary Logan Holley

April 8, 2019

Accepted by the faculty of the Department of Science and Mathematics, James Madison University, in partial fulfillment of the requirements for the Honors College.

FACULTY COMMITTEE:                                    HONORS COLLEGE APPROVAL:

Project Advisor:  George Vidal, Ph.D.,                Bradley R. Newcomer, Ph.D.,
Assistant Professor, Biology Department               Dean, Honors College

Reader:  Mark Gabriele, Ph.D.,
Professor, Biology Department

Reader:  Janet Daniel, Ph.D.,
Associate Professor, Biology Department

PUBLIC PRESENTATION

This work is accepted for presentation, in part or in full, at Society For Neuroscience on November 4, 2018.

## Dedication

I would like to dedicate this work to my Mom and Dad for their continuous love and support. I am eternally grateful for all you have done for me to allow me to have this opportunity.

## Table of Contents

# Acknowledgements

**Abstract**

Integrin subunits have been implicated in axonal and dendritic outgrowth. In particular, a strong positive association has been found between mutations in integrin beta 3 (*Itgb3*) and autism spectrum disorder, but little is known about neuronal *Itgb3* function in vivo. Many forms of autism spectrum disorder are thought to arise from dysfunctional dendritic arborization and synaptic pruning. Global knockout of *Itgb3* in mice leads to autistic-like behaviors. $Itgb3^{-/-}$ mice also have reduced callosal volume, a key neuroanatomical correlate of autism. Here, we test the hypothesis that *Itgb3* is required for normal dendritic arborization in layer II/III pyramidal neurons of mouse neocortex. This was achieved by causing *Itgb3* loss of function through Cre-lox-mediated excision of *Itgb3* in a subset of layer II/III cortical neurons. Layer II/III cortical neurons were targeted for excision via in utero electroporation of GFP/Cre DNA constructs to the ventricular zone of developing telencephalon of mice in which exon 1 of *Itgb3* is flanked by loxP sites. Laminar positioning, regional targeting, and dendritic arborization of targeted neurons in juvenile mice (P23) were analyzed. Male and female mice were used for the study and analysis was blind to genotype. Results point to aberrant basal dendritic arborization of mutant neurons, when compared to C57BL6/J controls. Thus, integrin beta 3 appears to regulate basal dendritic arborization of layer II/III pyramidal neurons in the developing neocortex.

**Introduction**

5

Many neurodevelopmental disorders, such as autism spectrum disorder (ASD), are thought to be associated with disorders of the synapse. ASD is often characterized by repetitive behaviors, deficits in communication, and overall impaired social interaction (American Psychiatric Association, 2013). Within the United States, this spectrum of disorders is thought to affect 1 in every 68 children over the age of 8 (Christensen *et al.*, 2016). ASD is accompanied by an excess of synapses formed by excitatory neurons within the cerebral cortex (Hutsler and Zhang, 2010; Tang *et* al., 2014). Normally, within early stages of development, individuals will overproduce synapses (Huttenlocher *et al.*, 1982). The synapses that are not necessary for normal brain function will then be rapidly pruned away, and the brain will reach relatively stable levels of synapses for the remainder of life (Grutzendler, Kasthuri, Gan, 2002). However, in individuals with ASD, there appears to be some problem with this pruning mechanism, which leads to a lasting excess of dendritic spines within the brain (Tang *et al.*, 2014). Many forms of ASD are believed to be caused by dysfunctional dendritic arborization and synaptic pruning (Hutsler and Zhang, 2010; Tang *et al.*, 2014). Dendritic arborization plays an important role in the development of the excitatory circuitry in the cortex, which is also important in ASD (He *et al.*, 2018; Nagode *et al.*, 2017).

Integrins are non-covalently-linked heterodimeric cell adhesion molecules comprised of an alpha and a beta subunit that bind to the extracellular matrix and regulate cell motility (Humphries, 2006). These molecules are required for normal

structural plasticity of dendrites and synapses, as well as for construction of cortical circuits within the brain (Thompson-Peer *et al.*, 2016). In neurons, beta subunits of integrins have been implicated in dynamic structural processes such as axonal and dendritic outgrowth (Kerrisk *et al.*, 2013; Warren *et al.*, 2012; Lin *et al.*, 2013), neuronal migration (Anton *et al.*, 1999; Pasterkamp *et al.*, 2003; Carlstrom *et al.*, 2011; Myers *et al.*, 2011), and dendritic spine plasticity (Shi and Ethell, 2006; Kramar *et al.*, 2006).

Despite the compelling amount of evidence of the positive association between ASD and mutations in integrin beta 3 (Weiss *et al.*, 2006; Coutinho *et al.*, 2007; Ma *et al.*, 2009; Napolioni *et al.*, 2011; O'Roak *et al.*, 2012; Singh *et al.*, 2013; Schuch *et al.*, 2014), little is known about the *in vivo* neuroanatomical function of integrin beta 3. Thus far, cellular studies have shown a neuronal function of *Itgb3* as it interacts directly with the GluA2 subunit of AMPA receptors in excitatory neurons (Cingolani *et al.*, 2008; Pozo *et al.*, 2012), but other potential neuroanatomical functions are unknown. Global knockout mice of *Itgb3* exhibited both autistic like behaviors (Carter *et al.*, 2011), as well as reduced volume of the corpus callosum (Ellegood *et al.*, 2012). Reduced callosal volume is a key neuroanatomical correlate of ASD (Egaas *et al.*, 1995; Frazier and Hardan, 2009; Freitag *et al.*, 2009; McAlonan *et al.*, 2009; Vidal CN *et al.*, 2006;). The axons of supragranular excitatory pyramidal neurons located in layer II/III of the six-layer cerebral cortex typically project from one hemisphere to the other through the corpus callosum (Leone *et al.*, 2008). As

ASD is thought to be partly due to dysfunctional dendritic arborization of excitatory neurons, and integrins have been implicated in this process, it is necessary to further examine the role *Itgb3* specifically plays within neuroanatomical development of supragranular excitatory neurons of layer II/III.

**Hypothesis**

We hypothesized that integrin beta 3 coordinates growth and arborization of excitatory neuronal dendrites of layer II/III of the cerebral cortex. In order to test this hypothesis, cell-specific loss of function of integrin beta 3 was analyzed within excitatory (layer II/III pyramidal) neurons of the somatosensory, auditory, and visual regions of the cerebral cortex of mice, given that these regions are associated with the abnormal sensory performance of individuals with ASD.

**Material and Methods**

**Ethics statement**

This study was carried out in accordance with the principles of the Basel Declaration and recommendations of the National Institutes of Health Office of Laboratory Animal Welfare, the United States Department of Agriculture, and the Guide for the Care and Use of Laboratory Animals of the United States National Research Council. The protocol was approved by the James Madison University Institutional Animal Care and Use Committee, Protocol A17-02.

**Data sets**

The reconstruction data for C57BL6/J;Cre[+] mice analyzed for this study are from a previously published study (Holley *et al.*, 2018) and will be uploaded and freely available on the NeuroMorpho.Org repository (NeuroMorpho.Org, RRID:SCR_002145; Ascoli *et al.*, 2007; Akram *et al.*, 2018).

**Overall experimental controls, transparency, and statistical methods**

Subjective bias was minimized by acquiring images blind to morphological characteristics and exact anatomical position. The experiment included a total of 125 pyramidal neurons from five brains, 78 neurons coming from three brains from the C57BL6/J line and 48 neurons coming from two brains from the *Itgb3^{fl/fl}* line, taken from five independent and complete replications of the experiment (*i.e.*, five mice, each from a different *in utero* electroporation surgery and thus from five different litters). These brains were selected for their broad rostrocaudal pattern of GFP expression. Statistical analysis (*e.g.*, linear regression) was performed using GraphPad Prism software (Graphpad Prism, RRID:SCR_002798). Shapiro-Wilk tests were used to test for a normal distribution. If the corresponding data passed

the Shapiro-Wilk normality test, a student's t-test with Welch's correction was used to compare the data sets. If the corresponding data sets did not pass the Shapiro-Wilk normality test, a Mann-Whitney t-test was used to compare the data sets. Quantifications of grouped data are presented as mean ± standard error of the mean. In all cases, P values were set with an alpha of 0.05.

**Experimental animals, husbandry, and housing**

The animals used in this experiment were female and male C57BL6/J and *Itgb3^{fl/fl}* mice derived from two lines of breeder pairs obtained from The Jackson Laboratory (IMSR cat. no. JAX:000664, RRID:IMSR_JAX:000664; IMSR cat. No. JAX:028232, RRID:IMSR_JAX:028232). After birth, the mice were housed with their parents and littermates until weaning (21 days after birth), and then with their same-sex littermates until the experimental endpoint (23 days after birth). Mice were housed in a temperature- and humidity-controlled, specific-pathogen-free environment with Teklad ¼" corncob bedding and were fed Teklad 18% protein rodent diet. The room housing the mice followed a 12-hour light/dark cycle. To generate timed-pregnant mice, females that had given birth and raised a litter successfully were paired with a male the day before the peak of estrus. Mice were then separated the next day. Thus, if the female was pregnant, the day the mice were separated would be counted as embryonic day 0.5 (E0.5).

**Deletion of *Itgb3* in mice**

To cause *Itgb3* loss of function, we targeted tissue that had loxP sites flanking (floxed) exon 1 of the *Itgb3* gene with DNA constructs that express Cre recombinase. When these DNA constructs entered mammalian cells, they caused excision of the floxed exon within that cell, and also expressed green fluorescent protein (GFP). This method allowed us to know that if a neuron is expressing GFP, then that cell has also expressed Cre recombinase and lost function of the *Itgb3* gene. The DNA constructs were amplified in *E. coli* and purified using standard microbiological techniques. Once the desired DNA construct concentration was attained, we injected the DNA construct into the lateral ventricle of the mouse embryos at embryonic day 15.5 using *in utero* electroporation (Vidal *et al.*, 2016; Bland *et al.*, 2017; Holley *et al.*, 2018). Electroporation at day E15.5 is critical, as electroporation on this day targets layer II/III neurons of the cerebral cortex (Saito T, Nakatsuji N, 2001).

**Delivery of DNA constructs via *in utero* electroporation**

To achieve sparse and bright labeling of supragranular neurons, the so-called "Supernova" system was used, in which a high concentration of a conditional enhanced green fluorescent protein (EGFP) construct and a low concentration of a Cre recombinase construct are co-electroporated; thus, the few cells that have the Cre recombinase construct are very likely to have multiple copies of the conditional EGFP construct (Mizuno *et al.*, 2014; Luo *et al.,* 2016). The conditional EGFP construct ("pK038.CAG-loxP-stop-loxP-EGFP-ires-tTA-WPRE (Supernova)", Addgene cat. no. 85006; Addgene, RRID:SCR_002037) and the Cre recombinase

construct ("pK031.TRE-Cre (Supernova)", AddGene cat. no. 69136; Addgene, RRID:SCR_002037) were gifts from Takuji Iwasato (http://snsupport.webcrow.jp/). Constructs were amplified using standard microbiological techniques, and purified using an EndoFree Maxi kit (QIAGEN, RRID:SCR_008539). Previously described protocols were followed in order to deliver the DNA constructs via *in utero* electroporation to label a sparse population of pyramidal neurons (Holley *et al.*, 2018; Vidal *et al.,* 2016; Bland *et al.,* 2017). In brief, a timed-pregnant mouse was deeply anesthetized at E15.5 using 1-2.5% isoflurane in 100% oxygen. An incision was made down the midline of the abdomen in order to expose the uterus. Once the uterus had been exposed, 1 μL of the DNA constructs (final concentrations of constructs: 1 mg/mL pK038.CAG-loxP-stop-loxP-EGFP-ires-tTA-WPRE (Supernova) and 10 μg/mL pK031.TRE-Cre (Supernova), in 1× phosphate-buffered saline) was injected into the lateral ventricle of each embryo using a calibrated pipette. Following the DNA construct injection, five 50 ms electrical pulses of 50 V with a 950 ms interval were delivered to each embryo using a square wave electroporation generator (ECM 830, BTX) and 5 mm platinum-plated tweezer-type electrodes (BTX) in order to facilitate the migration of the DNA into a broad swath of ventricular and subventricular zone progenitors fated to become layer II/III pyramidal neurons (Saito, 2006; Stancik *et al.*, 2010). The embryos and uterus were put back into their original position and the abdominal wall was sutured shut. Buprenorphine was administered intraperitoneally at 0.03 mg/kg, and the female

recovered in a separate cage for several hours. After recovery, the mouse was returned to its home cage, where it gave birth and raised its litter normally.

**Histology**

Three male (one *Itgb3fl/fl* and two C57BL6/J) and two female (one *Itgb3fl/fl* and one C57BL6/J) mice were transcardially perfused on postnatal day 23. An early age (postnatal day 23) was chosen because dendritic arbors are known to be plastic throughout life (Lee *et al.*, 2005; Chen *et al.*, 2011), yet an early critical period regarding dendritic arborization is largely complete by postnatal day 15 (Miller and Peters, 1981; Maravall *et al.*, 2004). Each mouse was first euthanized by peritoneal injection of a ketamine (240 mg/kg)-xylazine (48 mg/kg)-acepromazine (1.85 mg/kg) cocktail. Once the mouse no longer exhibited any toe pinch reflexes, 20 mL of ice-cold 1× phosphate-buffered saline (PBS) followed by 25 mL ice-cold, freshly made 4% paraformaldehyde, pH 7.4 (PFA) were transcardially perfused. The skull and brain were post-fixed in 4% PFA for 24 hours at 4 °C. After 24 hours, the solution was diluted to 1% PFA by adding 1× PBS, and stored for up to two weeks at 4 °C. The skull was removed from the 1% PFA solution and the brain was dissected from the skull. A coronal cut was made across the rostral end of the brain. The brain was then mounted rostral side down onto the stage of a vibrating microtome (Vibratome VT1000, Leica Microsystems). The Vibratome was then used to cut sequential 100 μm thick coronal sections. An important reason for taking coronal sections over tangential sections was to increase the amount of anatomical data acquired. *In utero* electroporation randomly targets a subset of neuronal progenitors.

Consequently, it is impossible to pre-select dendritic arbors to all be confined to a specific tangential slice. Therefore, in this case, the best sectioning plane for maximum data acquisition per brain was coronal, because it was not anticipated exactly which layer II/III neurons would be labeled. In previous experiments, a DAPI stain was used to confirm that labelled neurons were located within layer II/III. Another advantage of taking coronal sections was that the apical dendritic arbors were preserved, in addition to the basal dendritic arbors. To increase the portion of the basal arbor sampled in our study, we took 100 μm sections (thicker sections would have resulted in light scatter during confocal microscopy, confounding results). Sections were mounted on glass slides with Prolong Diamond Antifade Mountant (Life Technologies) and cured for 24 hours in the dark. The slides were then sealed with melted VALAP (equal parts Vaseline, lanolin, and paraffin).

**Anatomical positioning data acquisition and analysis**

Prepared slides were scanned for green fluorescent protein (GFP) at low magnification (4×) using a Nikon Eclipse Ti2 fluorescence microscope. If cells containing GFP were identified, a 4× automatically-stitched image of the entire coronal section containing the cell was then taken using the microscope and a Hamamatsu ORCA-Flash4.0 C13440 digital camera. Using FIJI software (Fiji, RRID:SCR_002285), cortical depth and distance-to-midline was determined by measuring $(x,y)$ distances from the center of the soma radially out to the pial surface of the cortex (cortical depth), and from the center of the soma on the $x$-axis to the

midline of the coronal section (distance-to-midline). Each coronal image was compared to the 2008 Allen Mouse Brain Reference Atlas as well as a developing mouse brain atlas (Lein *et al.*, 2007; http://mouse.brain-map.org/static/atlas; Paxinos *et al.*, 2006) to determine the cortical region of each neuron by matching neuroanatomical landmarks and distances from the atlas to the 4× images; although shrinkage or swelling of the tissue was not observed with this histological technique, the mediolateral and dorsoventral axes of the section and the atlas were aligned and standardized to each other to account for any effects of tissue processing. Once the cortical region was determined, the distance to the closest cortical region was measured using the scale on the reference atlas. Only neurons with a high confidence of being in a cortical region (> 0.25 mm distance to closest cortical region) were used for inter-regional analysis, while all other analyses were blind to putative regional identity.

**Dendritic morphological data acquisition and analysis**

Using a Nikon Eclipse TE2000-E confocal microscope, Z-stack images of the full field of view were taken at 20× magnification of the complete (apical and basal) dendritic arbor from the same GFP-positive cells that were analyzed at 4× magnification. Images were taken at or above the Nyquist sampling rate in the z-direction. These Z-stack images were then used to create semi-automated 3D reconstructions of each neuron utilizing the software neuTube (Feng *et al.*, 2015). Using the Simple Neurite Tracer plugin for FIJI (Longair *et al.*, 2011), each path of the reconstructed neuron was assigned as being a part of the soma, the apical

16

dendrite, or a basal dendrite. Using the assigned paths and the software L-Measure (L-Measure, RRID:SCR_003487; Scorcioni *et al.*, 2008), the functions *N_stems* (number of primary dendrites), *N_bifs* (number of bifurcations in the dendritic arbor), *N_tips* (number of dendritic endings), and *length* (dendritic length) were measured for the apical and basal dendrites, respectively. The Sholl Analysis function within FIJI (Ferreira *et al.*, 2014) was used for both apical and basal dendrites in order to determine the number of intersections at each distance from the soma. In addition to these classic parameters (Sholl, 1953), the mean value of the polynomial function used by the software to fit the Sholl analysis plot was used as a way to evaluate the average number of intersections made by the apical and basal arbors, respectively.

# Results

To determine whether *Itgb3* expression within excitatory pyramidal neurons is required for normal dendritic morphology, C57BL6/J;Cre⁺ and *Itgb3ᶠˡ/ᶠˡ*;Cre⁺ mice were studied using *in utero* electroporation of GFP;Cre constructs to target a subset of isochronically-sourced layer II/III excitatory pyramidal neurons at the time of their genesis. One construct consisted of a Tetracycline Response Element (TRE)-Cre recombinase sequence, and the other consisted of a CAG-loxP-stop-loxP-GFP-Tetracycline trans-activator (tTA) sequence. When both constructs are present within a neuron, leaky Cre expression reaches a certain threshold within a neuron and the stop sequence is excised from the other construct, leading to the expression of both GFP and tTA (Luo *et al.*, 2016). These constructs then act in a positive feedback manner leading to high levels of expression of both GFP and Cre recombinase. Whenever Cre recombinase is expressed within a cell that has a floxed gene, Cre recombinase will excise that specific gene, rendering it non-functional within that cell. However, the surrounding cells that do not contain both constructs will not have the floxed gene excised, and the gene is therefore functional within the cell. Therefore, cells that have had *Itgb3* excised are surrounded by wild-type tissue, allowing for the study of cell-specific phenotypes (Luo *et al.*, 2016).

Utilizing *in utero* electroporation provided several experimental advantages. First, this approach provided a way to limit selection bias as only excitatory pyramidal neurons that possessed both constructs would express GFP, and therefore all sufficiently-labeled neurons could be analyzed. Second, by choosing the date of electroporation, sets of neuronal precursors that are highly restricted in their

laminar fate to become layer II/III neurons could be targeted (Frantz and McConnell, 1996; Desai and McConnell, 2000; Shen *et al.*, 2006). Third, this technique preferentially targets cells in the S- and M-phase cells of the ventricular and subventrical zones (Stancik *et al.*, 2010), allowing us to target isochronically-sourced neurons— that is, neurons derived from progenitors that were dividing on the same day. Last, new developments in the technique (Holley *et al.*, 2018; Vidal *et al.*, 2016; Bland *et al.*, 2017) and in DNA constructs specifically made with the technique in mind (Mizuno *et al.*, 2014; Luo *et al.,* 2016), allowed us to target sparse populations of neurons while keeping a high-contrast GFP label that would permit accurate morphological reconstructions. We targeted a large area of the developing ventricular and subventricular zones at embryonic day 15.5 and observed the dendritic morphology of neurons from both mouse lines on postnatal day 23, allowing sufficient time for activity-dependent cues to have their major effect on the arborization of these neurons (McAllister, 2000; Cline, 2001; Wong and Ghosh, 2002; Pratt *et al.*, 2016), which occurs by postnatal day 15 (Miller and Peters, 1981; Maravall *et al.*, 2004).

**Sparse deletion of *Itgb3* in layer II/III neurons is correlated with elevated total dendritic length in mutant neurons compared to controls**

The first experiment was designed to determine whether dendritic arborization of layer II/III neurons in *Itgb3^{fl/fl}*;Cre^+ mice is altered at P23. At E15.5, C57BL6/J and *Itgb3^{fl/fl}* embryos were injected with a DNA construct (GFP;Cre) expressing GFP, as

well as Cre recombinase under a separate promoter and subjected to electroporation.

Electroporation at E15.5 results in laminar-specific GFP labeling of layer II/III pyramidal neurons throughout the targeted area of the cortex at P23 (Fig. 1A-B). Dendritic arbors were extensively labeled with GFP, as seen using confocal microscopy (Fig. 1C-D), permitting accurate morphological reconstruction and analysis. Total dendritic length in $Itgb3^{fl/fl}$;Cre$^+$ mice is significantly elevated by 15% compared to C57BL6/J;Cre$^+$ mice (Fig. 1E-F).
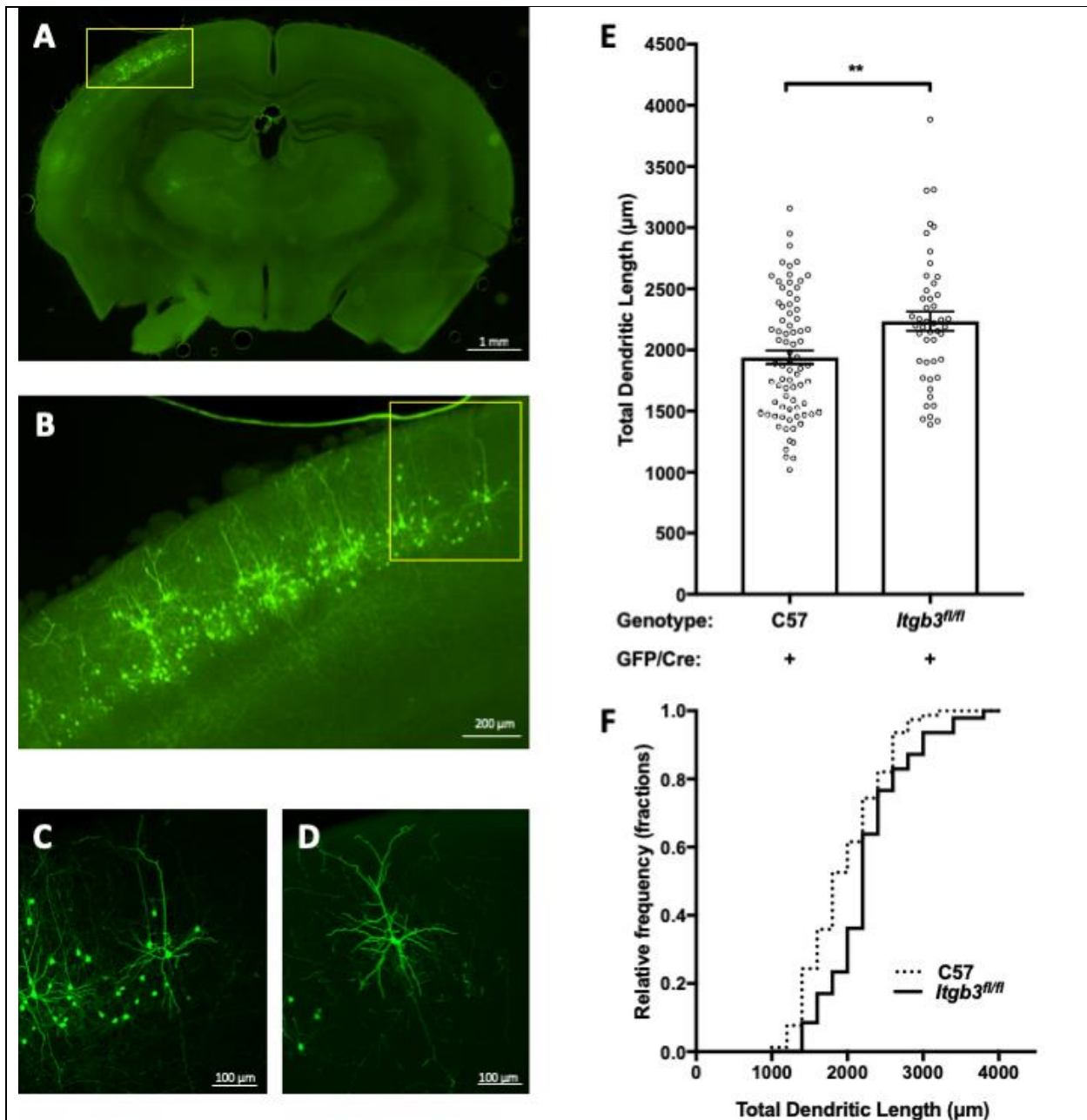
**Figure 1. Total dendritic length of layer II/III pyramidal neurons is greater in *Itgb3$^{fl/fl}$*;Cre$^{+}$ neurons than in C57;Cre$^{+}$ at postnatal day 23 (P23). (A).** Example of a low-magnification (4x) image of a coronal section from a C57;Cre$^{+}$ mouse. **(B).** Magnified view of the inset in (A), showing the general area of GFP labeling in this section. **(C).** Medium-magnification (20x) maximum intensity Z-projection of a confocal image of the cell in the inset in (B). **(D).** Medium-magnification (20x) maximum intensity Z-projection of a confocal image of a *Itgb3$^{fl/fl}$*;Cre$^{+}$ neuron. **(E).** Total dendritic length of layer II/III *Itgb3$^{fl/fl}$*;Cre$^{+}$ pyramidal neurons is elevated compared to C57;Cre$^{+}$ neurons (C57;Cre$^{+}$: 1940.0 ± 78.56 μm, n=78 neurons, 3 mice; *Itgb3$^{fl/fl}$*;Cre$^{+}$: 2235.0 ± 78.56 μm, n=47 neurons, 2 mice, p=0.0029, Student's t-test with Welch's correction). **(F).** Cumulative histogram (by cell) of data presented in (E).

**Layer II/III pyramidal neurons lacking *Itgb3* and developing in a sea of wild-type neurons have elevated basal, but not apical dendritic length**

After observing the significant increase in total dendritic length in *Itgb3*$^{fl/fl}$;Cre$^+$ mice, we wished to understand if this difference was restricted within a certain dendritic compartment (e.g. apical vs. basal dendrites). In order to answer this question, the apical and basal dendritic lengths of both *Itgb3*$^{fl/fl}$;Cre$^+$ mice and C57BL6/J;Cre$^+$ mice were each compared separately.

The total basal dendritic length of *Itgb3*$^{fl/fl}$;Cre$^+$ mice was 19% greater than that of C57BL6/J;Cre$^+$ mice (Fig. 2B). However, no significant difference was seen between total length of *Itgb3*$^{fl/fl}$;Cre$^+$ mice apical dendrites vs C57BL6/J;Cre$^+$ mice apical dendrites (Fig. 2A). Other apical morphological characteristics, such as the number of branch points (bifurcations), the number of dendritic endings (tips), and the number of crossings at each distance from the soma (Sholl) were also analyzed, similarly with no statistically significant differences being found (Supplemental Table 1).

**Figure 2. While apical dendritic length of layer II/III neurons is unaltered in *Itgb3fl/fl*;Cre⁺ neurons at P23, basal dendritic length of layer II/III neurons is significantly elevated. (A).** Apical dendritic length of layer II/III neurons is unaltered in *Itgb3fl/fl*;Cre⁺ compared to C57;Cre⁺ neurons (C57;Cre⁺: 833.8 ± 30.54 μm, n=78 neurons, 3 mice; *Itgb3fl/fl*;Cre⁺: 918.6 ± 53.86 μm, n=47 neurons, 2 mice, p=0.2914, Mann-Whitney test). **(B).** Basal dendritic length of layer II/III neurons in *Itgb3fl/fl*;Cre⁺ mice is elevated compared to layer II/III neurons in C57;Cre⁺ neurons (C57;Cre⁺: 1106.0 ± 44.82 μm, n=78 neurons, 3 mice; *Itgb3fl/fl*;Cre⁺: 1317.0 ± 56.11 μm, n=47 neurons, 2 mice, p=0.0042, Student's t-test with Welch's correction).

**Neurons lacking *Itgb3* and developing amongst wild-type neurons have more basal bifurcations and tips, but not primary basal dendrites, compared to control neurons**

The altered basal dendritic length led us to wonder what specific morphological characteristics were being modified to result in abnormally long total basal dendritic length. One possible explanation for greater basal dendritic length is that the mutant cell's basal dendrites have more branches than control cells, resulting in higher dendritic length. Another possible explanation for greater basal dendritic length is that mutant cells have a larger number of primary basal dendrites emanating from the soma but have the same number of branches as control cells. The third potential explanation for greater basal dendritic length is that mutant cells have the same number of primary basal dendrites and branches as control cells, but their dendrites are just longer than those of control cells. To test each of these explanations, we compared the number of primary basal dendrites, basal bifurcations, and basal tips for $Itgb3^{fl/fl}$;Cre$^+$ and C57BL6/J;Cre$^+$ neurons.

No significant difference was seen between basal primary dendrites of $Itgb3^{fl/fl}$;Cre$^+$ neurons vs C57BL6/J;Cre$^+$ neurons (Fig. 3A). However, $Itgb3^{fl/fl}$;Cre$^+$ neurons had significantly more basal bifurcations (37% more) than C57BL6/J;Cre$^+$ neurons (Fig. 3B). $Itgb3^{fl/fl}$;Cre$^+$ neurons also exhibited significantly more basal tips (16% more) than C57BL6/J;Cre$^+$ mice (Fig. 3C).
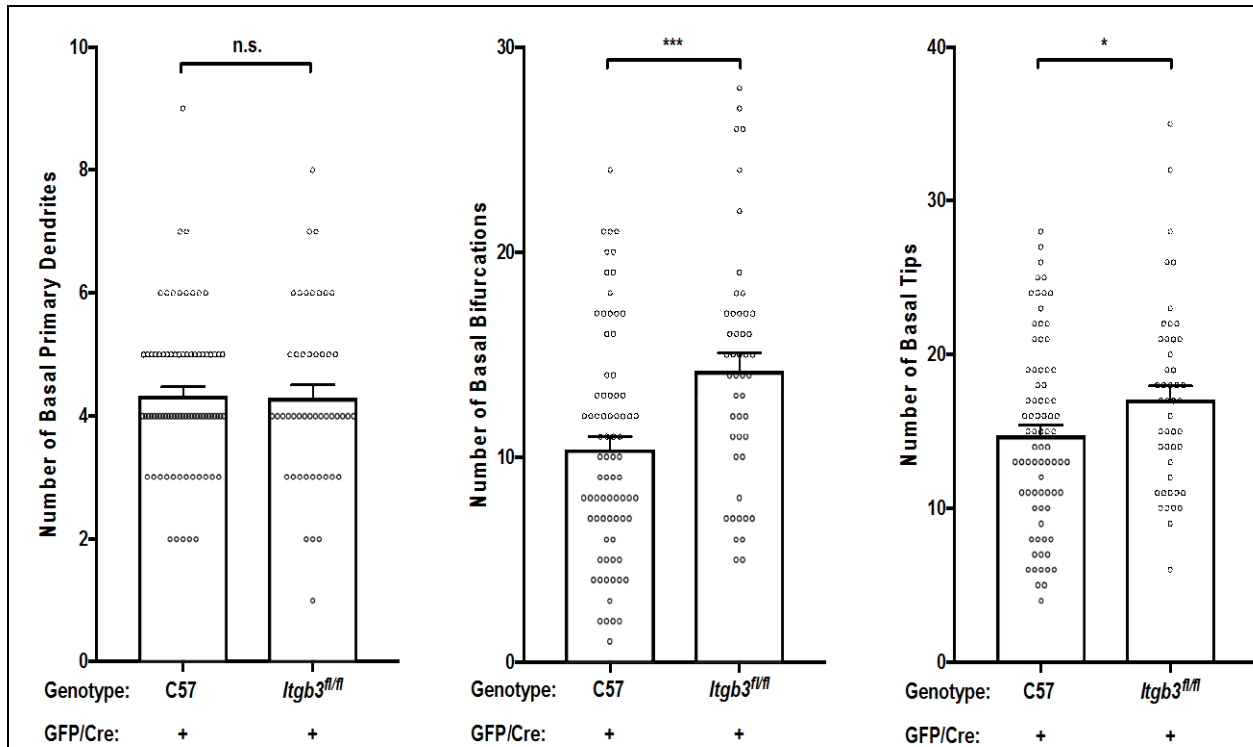
**Figure 3. While basal primary dendrites are unaltered, basal bifurcations and tips are both elevated in *Itgb3$^{fl/fl}$*;Cre$^+$ compared to C57;Cre$^+$ neurons. (A).** Basal primary dendrites of layer II/III *Itgb3$^{fl/fl}$*;Cre$^+$ neurons are unaltered compared to C57;Cre$^+$ neurons (C57;Cre$^+$: 4.333 ± 0.141, n=78 neurons, 3 mice; *Itgb3$^{fl/fl}$*;Cre$^+$: 4.298 ± 0.2105, n=47 neurons, 2 mice, p=0.8162, Mann-Whitney test). **(B).** *Itgb3$^{fl/fl}$*;Cre$^+$ basal dendrites have more bifurcations than C57;Cre$^+$ neurons (C57;Cre$^+$: 10.38 ± 0.6113, n=78 neurons, 3 mice; *Itgb3$^{fl/fl}$*;Cre$^+$: 14.21 ± 0.8554, n=47 neurons, 2 mice, p=0.0007, Mann-Whitney test). **(C).** *Itgb3$^{fl/fl}$*;Cre$^+$ basal dendrites have more tips than C57;Cre$^+$ neurons (C57;Cre$^+$: 14.74 ± 0.6805, n=78 neurons, 3 mice; *Itgb3$^{fl/fl}$*;Cre$^+$: 17.09 ± 0.8825, n=47 neurons, 2 mice, p=0.0382, Student's t-test with Welch's correction).

# Discussion

Here we show that *Itgb3* is required for normal dendritic arborization, an important process in the development of excitatory cortical circuits. More specifically, *Itgb3* is required for normal basal dendritic arborization but not for normal apical arborization. In basal dendritic development, *Itgb3* is required for normal branching but not for the normal development of primary basal dendrites.

There are several possible explanations as to why *Itgb3* is needed for certain aspects of normal dendritic development but not for others. One possible explanation is that *Itgb3* is not expressed within apical dendrites at all and is only expressed within the branch points of basal dendrites and not in the primary basal dendrites—in other words, apical dendritogenesis and basal dendritogenesis may occur utilizing two different sets of molecular machinery.  To test these ideas, a possible experiment would be to observe the expression of *Itgb3* throughout the neuron via immunohistochemistry of a supragranular excitatory pyramidal neuron that is fully expressing *Itgb3* and assess the localization of Itgb3 throughout the neuron's soma and dendrites.

It may be that *Itgb3* is important for other aspects of dendritic development earlier or later in development. Since we focused our experiment at P23, after dendritic arborization is normally complete, we cannot conclude about the requirement of *Itgb3* in normal dendritic development before or after P23. In order to test the requirement for *Itgb3* throughout development, more replications of our experiment

could be done at earlier developmental times and later developmental times to see if there are differences in the anatomical features of neurons, when compared to controls.

By having a greater total dendritic length and more branches, the basal dendrites of *Itgb3*$^{fl/fl}$;Cre$^+$ neurons potentially have greater total excitatory connectivity compared to controls if they have the same or higher density of excitatory synaptic inputs. We have gathered preliminary data that have shown the dendritic spine density—an indirect measure of excitatory synaptic inputs onto a pyramidal neuron (there is a synapse present over 95% at each dendritic spine; Arellano *et al.*, 2007) —of *Itgb3*$^{fl/fl}$;Cre$^+$ is unchanged compared to controls. Assuming this is correct and that each dendritic spine is in fact forming a synapse, this would imply that *Itgb3*$^{fl/fl}$;Cre$^+$ neurons have greater total excitatory connectivity. In conjuncture with the indirect measurement of spine density as a correlate for excitatory connectivity, another indirect measure must be utilized to corroborate the results. For example, one indirect physiological correlate of excitatory connectivity is the frequency of mini excitatory post-synaptic currents (mEPSC). By blocking action potentials from pre-synaptic neurons and NMDA receptors on the post-synaptic neuron, the frequency of AMPA receptor activation on a given neuron can be isolated. The frequency of AMPA receptor activation for mutant neurons can then be compared to control neurons to assess whether or not differences in spine density are also correlated with a difference in the total functional connectivity of these neurons. A

direct measure of synaptic connectivity, such as immunogold electron microscopy, could be used to assess both dendritic spine density and synapse density. Labeling GFP+ cells with an antibody conjugated to gold particles makes the labeled neuron electron dense, thereby revealing the cell's ultrastructure (including whether or not a dendritic spine is part of a synapse).

By using *in utero* electroporation of the Supernova system, we are able to analyze the cell-specific loss-of-function of *Itgb3* and how this alters the anatomy of supragranular excitatory pyramidal neurons lacking *Itgb3* in a sea of wild-type neurons. Since neuronal morphology is influenced by the inputs of surrounding neurons, this allows us to see how not having functional *Itgb3* within a neuron alters its morphology while it still receives input from neurons with functional *Itgb3*. However, it is unknown whether or not the cell lacking Itgb3 has any similar effects on surrounding neurons. If the cell lacking Itgb3 does not have any effect on surrounding neurons, then the function of Itgb3 in dendritic arborization is cell-autonomous. However, if the cell lacking Itgb3 does have an effect on surrounding neurons, then Itgb3 may have an additional, non-cell-autonomous function. To distinguish between these possibilities, it is necessary for us to observe the cells surrounding mutant neurons, using either a reporter mouse or immunohistochemistry. If the loss of *Itgb3* does not alter the morphology of the surrounding neurons, this would reinforce the idea that we are actually analyzing the cell-autonomous functions of *Itgb3*.

The dendritic arborization of supragranular excitatory pyramidal neurons is an important aspect of the formation of cortical circuits and is related to autism spectrum disorder. By assessing and comparing the morphology of mutant neurons lacking *Itgb3* with control neurons, we have found that this gene is required for the normal development of basal dendrites. Knowing the exact location and function of *Itgb3* in the developing cortical circuitry can lead us closer to a mechanism for how problems in *Itgb3* expression can lead to autism.

**Author Contributions**

Portions of this study were published as Holley *et al.* (2018). This study originated from early discussions among Logan Holley, Kate Bland, Zach Casey, Chris Handwerk and Dr. George Vidal, which arose from data acquired by all contributors. LH, KB, ZC, CH, and GV completed experiments and acquired data; most experimentation and data acquisition was done by LH. LH and ZC organized the database. LH and GV analyzed the data. LH wrote the thesis under the mentorship of GV.

**Supplementary Information**

**Supplemental Table 1. Anatomical homogeneity of features of mouse supragranular excitatory pyramidal neurons between C57BL6/J;Cre[+] and *Itgb3^{fl/fl};Cre[+] lines.***

| | C57 Mean | C57 SEM | ITGB3 Mean | ITGB3 SEM | p |
|---|---|---|---|---|---|
| Apical Bifurcations | 7.679 | 0.3777 | 8.787 | 0.6044 | 0.2181 |
| Apical Tips | 8.628 | 0.3828 | 9.426 | 0.632 | 0.5060 |
| Apical Sholl Mean Value | 2.872 | 0.0944 | 2.96 | 0.132 | 0.7005 |

A non-parametric Mann-Whitney test showed no statistically significant differences in the anatomical features of C57BL6/J;Cre[+] and *Itgb3^{fl/fl};Cre[+]* supragranular excitatory pyramidal neurons.

**Supplemental Table 2. Differences in anatomical features of mouse supragranular excitatory pyramidal neurons located within the primary somatosensory functional cortical region between C57BL6/J;Cre$^+$ and *Itgb3$^{fl/fl}$;Cre$^+$ lines.***

| | C57 Mean | C57 SEM | ITGB3 Mean | ITGB3 SEM | p |
|---|---|---|---|---|---|
| SSp Total Dendritic Length (μm) | 1911 | 68.45 | 2223 | 89.13 | 0.0086 |
| SSp Apical Bifurcations | 7.564 | 0.4198 | 9.028 | 0.7669 | 0.2325 |
| SSp Apical Tips | 8.545 | 0.4223 | 9.778 | 0.7969 | 0.3857 |
| SSp Apical Length (μm) | 841.3 | 34.77 | 939.9 | 65.91 | 0.3420 |
| SSp Apical Sholl Mean Value | 2.919 | 0.1163 | 2.93 | 0.1548 | 0.9533 |
| SSp Basal Primary Dendrites | 4.145 | 0.15 | 4.167 | 0.2567 | 0.7916 |
| SSp Basal Bifurcations | 9.836 | 0.7827 | 14.08 | 0.9507 | 0.0008 |
| SSp Basal Tips | 14.0 | 0.8681 | 16.81 | 1.036 | 0.0371 |
| SSp Basal Length (μm) | 1070.0 | 56.83 | 1283.0 | 59.38 | 0.0129 |
| SSp Basal Sholl Mean Value | 5.802 | 0.327 | 6.891 | 0.4433 | 0.0328 |

A non-parametric Mann-Whitney test showed statistically significant differences in the total dendritic length, number of basal bifurcations, number of basal tips, basal dendritic length, and basal sholl mean value between C57BL6/J;Cre$^+$ and

*Itgb3fl/fl;Cre+* neurons located within the primary somatosensory functional region. In order to reassure that neurons were within their assigned cortical functional region, only neurons over 0.25mm from the border of another region were used for regional analysis. Sholl Mean Value is the mean value of the fitted polynomial function over a Sholl profile, representing the average of intersections over the whole area occupied by the arbor (see Methods).

# References

Akram, M. A., Nanda, S., Maraver, P., Armañanzas, R., and Ascoli, G. A. (2018). An open repository for single-cell reconstructions of the brain forest. Scientific Data 5, 180006. doi:10.1038/sdata.2018.6.

American Psychiatric Association. Diagnostic and statistical manual of mental disorders. 5th ed. Text revision. Washington, DC: American Psychiatric Association; 2013.

Anton, E. S., Kreidberg, J. A., and Rakic, P. (1999). Distinct functions of alpha3 and alpha(v) integrin receptors in neuronal migration and laminar organization of the cerebral cortex. Neuron 22(2):277-89. PMID: 10069334.

Arellano, J. I., Espinosa, A., Fairén, A., Yuste, R., and DeFelipe, J. (2007). Non-synaptic dendritic spines in neocortex. Neuroscience 145, 464–469. doi:10.1016/j.neuroscience.2006.12.015.

Ascoli, G. A., Donohue, D. E., and Halavi, M. (2007). NeuroMorpho.Org: A Central Resource for Neuronal Morphologies. Journal of Neuroscience 27, 9247–9251. doi:10.1523/jneurosci.2055-07.2007.

Bland, K., Casey, Z. O., Handwerk, C. J., Holley, Z. L., and Vidal, G. S. (*2017*). Inducing Cre-lox Recombination in Mouse Cerebral Cortex Through *in Utero* Electroporation. J Vis Exp.

Carlstrom, L. P., Hines, J. H., Henle, S. J., and Henley, J. R. (2011). Bidirectional remodeling of ß1-integrin adhesions during chemotropic regulation of nerve growth. BMC Biol 9:82. PMCID: PMC3283487.

Carter, M. D., Shah, C. R., Muller, C. L., Crawley, J. N., Carneiro, A. M., and
Veenstra-Vanderweele, J. (2011). Absence of preference for social novelty and
increased grooming in integrin ß3 knockout mice: initial studies and future
directions. Autism Res. 4(1), 57-67.

Chen, J. L., Lin, W. C., Cha, J. W., SO, P. T., Kubota, Y., and Nedivi, E. (2011)
Structural Basis for the Role of Inhibition in Facilitating Adult Brain
Plasticity. Nature Neuroscience 14, 587-594. Doi: 10.1038/nn.2799

Christensen, D. L., Baio, J., Van Naarden Braun, K., Bilder, D., Charles, J.,
Constantino, J. N., Daniels, J., et al (2016). Prevalence and Characteristics of
Autism Spectrum Disorder Among Children Aged 8 Years--Autism and
Developmental Disabilities Monitoring Network, 11 Sites, United States,
2012. MMWR Surveil Summ 65(3):1-23. PMID: 27031587.

Cingolani, L. A, Thalhammer, A., Yu, L. M., Catalano, M., Ramos, T., Colicos, M. A.,
and Goda, Y. (2008). Activity-dependent regulation of synaptic AMPA
receptor composition and abundance by beta3 integrins. Neuron 58(5):749-62.
PMCID: PMC2446609.

Cline, H. T. (2001). Dendritic Arbor Development and Synaptogenesis. Current
Opinion in Neurobiology 11, 118-126.

Coutinho, A. M., Sousa, I., Martins, M., Correia, C., Morgadinho, T., Bento, C., and
Vincente, A. M. (2007). Evidence for epistasis between SLC6A4 and ITGB3 in
autism etiology and in the determination of platelet serotonin levels. Hum
Genet. 121(2), 243-56.

Desai, A. R., and McConnell, S. K. (2000). Progressive restriction in fate potential by neural progenitors during cerebral cortical development. Development 127, 2863-2872.

Egaas, B., Courchesne, E., and Saitoh, O. (1995). Reduced size of corpus callosum in autism. Arch Neurol 52(8):794-801. PMID: 7639631.

Ellegood, J., Henkelman, R. M., and Lerch, J. P. (2012). Neuroanatomical Assessment of the Integrin β3 Mouse Model Related to Autism and the Serotonin System Using High Resolution MRI. Front Psychiatry. 3, 37.

Feng, L., Zhao, T., and Kim, J. (2015). neuTube 1.0: A New Design for Efficient Neuron Reconstruction Software Based on the SWC Format. eNeuro 2. doi:10.1523/eneuro.0049-14.2014.

Ferreira, T. A., Blackman, A. V., Oyrer, J., Jayabal, S., Chung, A. J., Watt, A. J., *et al.* (2014). Neuronal morphometry directly from bitmap images. Nature Methods 11, 982–984. doi:10.1038/nmeth.3125.

Frantz, G. D., and McConnell, S. K. (1996). Restriction of Late Cerebral Cortical Progenitors to an Upper-Layer Fate. Neuron 17, 55-61.

Frazier, T. W. and Hardan, A. Y. (2009). A meta-analysis of the corpus callosum in autism. Biol Psychiatry. 66(10), 935-941.

Freitag, C. M., Luders, E., Hulst, H. E., Narr, K. L., Thompson, P. M., Toga, A. W., Krick, C., and Konrad, C. (2009). Total brain volume and corpus callosum size in medication-naïve adolescents and young adults with autism spectrum disorder. Biol Psychiatry 66(4):316-9. PMCID: PMC3299337.

Grutzendler, J., Kasthuri, N., and Gan, W. B. (2002). Long-term dendritic spine stability in the adult cortex. Nature 420, 812-816.

He, H., Shen, W., Zheng, L., Guo, X., and Cline, H. T. (2018). Excitatory synaptic dysfunction cell-autonomously decreases inhibitory inputs and disrupts structural and functional plasticity. Nature Communications 9. doi:10.1038/s41467-018-05125-4.

Holley, Z. L., Bland, K. M., Casey, Z. O., Handwerk, C. J., and Vidal, G. S. (2018) Cross-Regional Gradient of Dendritic Morphology in Isochronically-Sourced Mouse Supragranular Pyramidal Neurons. Front. Neuroanat. 12:103. doi: 10.3389/fnana.2018.00103

Humphries, J. D. (2006). Integrin ligands at a glance. Journal of Cell Science 119, 3901–3903. doi:10.1242/jcs.03098.

Hutsler, J. J. and Zhang, H. (2010). Increased dendritic spine densities on cortical projection neurons in autism spectrum disorders. Brain Res. 1309, 83-94.

Huttenlocher, P. R., de Courten, C., Garey, L. J., and Van der Loos, H. (1982). Synaptogenesis in human visual cortex--evidence for synapse elimination during normal development. Neurosci Lett 33:247-52.

Kerrisk, M. E., Greer, C. A., and Koleske, A. J. (2013). Integrin α3 is required for late postnatal stability of dendrite arbors, dendritic spines and synapses, and mouse behavior. J Neurosci 33(16):6742-52. PMCID: PMC3711182.

Kramár, E. A., Lin, B., Rex, C. S., Gall, C. M., and Lynch, G. (2006). Integrin-driven
actin polymerization consolidates long-term potentiation. PNAS. 103(14),
5579-5584.

Lee, W.-C. A., Huang, H., Feng, G., Sanes, J. R., Brown, E. N., So, P. T., *et al.*
(2005). Dynamic Remodeling of Dendritic Arbors in GABAergic Interneurons
of Adult Visual Cortex. PLoS Biology 4, e29.
doi:10.1371/journal.pbio.0040029.

Lein, E. S., Hawrylycz, M. J., Ao, N., Ayres, M., Bensinger, A., Bernard, A., *et al.*
(2006). Genome-wide atlas of gene expression in the adult mouse brain.
Nature 445, 168–176. doi:10.1038/nature05453.

Leone, D. P., Srinivasan, K., Chen, B., Alcamo, E., and McConnell, S. K. (2008). The
determination of projection neuron identity in the developing cerebral cortex.
Current Opinion in Neurobiology 18(1): 28-35. doi:10.1016/j.conb.2008.05.006

Lin, Y. C., Yeckel, M. F., and Koleske, A. J. (2013). Abl2/Arg controls dendritic spine
and dendrite arbor stability via distinct cytoskeletal control pathways. J
Neurosci 33(5):1846-57. PMCID: PMC3711664.

Longair, M. H., Baker, D. A., and Armstrong, J. D. (2011). Simple Neurite Tracer:
open source software for reconstruction, visualization and analysis of
neuronal processes. Bioinformatics 27, 2453–2454.
doi:10.1093/bioinformatics/btr390.

Luo, W., Mizuno, H., Iwata, R., Nakazawa, S., Yasuda, K., Itohara, S., and Iwasato, T. (2016). Supernova: A Versatile Vector System for Single-Cell Labeling and Gene Function Studies in vivo. Sci Rep 6:35747. PMCID: PMC5075795.

Ma, D. Q., Rabionet, R., Konidari, I., Jaworski, J., Cukier, H. N., Wright, H. H., Abramson, R. K., et al (2010). Association and gene-gene interaction of SLC6A4 and ITGB3 in autism. Am J Med Genet B Neuropsychiatr Genet 153B(2):477-483. PMCID: PMC3735126.

Maravall, M., Koh I. Y., Lindquist W. B., and Svoboda K. (2004). Experience-dependent Changes in Basal Dendritic Branching of Layer 2/3 Pyramidal Neurons During a Critical Period for Developmental Plasticity in Rat Barrel Cortex. Cerebral Cortex 14, 655–664. doi:10.1093/cercor/bhh026.

McAllister, A. K. (2000). Cellular and Molecular Mechanism of Dendrite Growth. Cerebral Cortex 10, 963-973.

McAlonan, G. M., Cheung, C., Cheung, V., Wong, N., Suckling, J., and Chua, S. E. (2009). Differential effects on white-matter systems in high-functioning autism and Asperger's syndrome. Psychol Med 39(11):1885-93. PMID: 19356262.

Miller, M., and Peters, A. (1981). Maturation of Rat Visual Cortex. II. A Combined Golgi-Electron Microscope Study of Pyramidal Neurons. The Journal of Comparative Neurology 203, 555-573.

Mizuno, H., Luo, W., Tarusawa, E., Saito, Y. M., Sato, T., Yoshimura, Y., Itohara, S., and Iwasato, T. (2014). NMDAR-regulated dynamics of layer 4 neuronal

dendrites during thalamocortical reorganization in neonates. Neuron 82(2):365-79. PMID: 24685175.

Myers, J. P., Santiago-Medina, M., and Gomez, T. M. (2011). Regulation of axonal outgrowth and pathfinding by integrin-ECM interactions. Dev Neurobiol 71(11):901-23. PMCID: PMC3192254.

Nagode, D. A., Meng, X., Winkowski, D. E., Smith, E., Khan-Tareen, H., Kareddy, V., et al. (2017). Abnormal Development of the Earliest Cortical Circuits in a Mouse Model of Autism Spectrum Disorder. Cell Reports 18, 1100–1108. doi:10.1016/j.celrep.2017.01.006.

Napolioni, V., Lombardi, F., Sacco, R., Curatolo, P., Manzi, B., Alessandrelli, R., Militerni, R., et al (2011). Family-based association study of ITGB3 in autism spectrum disorder and its endophenotypes. Eur J Hum Genet 19(3):353-9. PMCID: PMC3062005.

O'Roak, B. J., Vives, L., Girirajan, S., Karakoc, E., Krumm, N., Coe, B. P., Levy, R., et al (2012). Sporadic autism exomes reveal a highly interconnected protein network of de novo mutations. Nature 485(7397):246-50. PMCID: PMC3350576.

Pasterkamp, R. J., Peschon, J. J., Spriggs, M. K., and Kolodkin, A. L. (2003). Semaphorin 7A promotes axon outgrowth through integrins and MAPKs. Nature 424(6947):398-405. PMID: 12879062.

Paxinos, G., Halliday, G. M., Watson, C., Koutcherov, Y., and Wang, H. (2006). Atlas of the Developing Mouse Brain at E17.5, P0, and P6.

Pozo, K., Cingolani, L. A., Bassani, S., Laurent, F., Passafaro, M., and Goda, Y. (2012). β3 integrin interacts directly with GluA2 AMPA receptor subunit and regulates AMPA receptor expression in hippocampal neurons. Proc Natl Acad Sci U S A 109(4):1323-8. PMCID: PMC3268285.

Pratt, K. G., Hiramoto, M., and Cline, H. T. (2016). An Evolutionarily Conserved Mechanism for Activity-Dependent Visual Circuit Development. Frontiers in Neural Circuits 10. doi:10.3389/fncir.2016.00079.

Saito, T. (2006). In vivo electroporation in the embryonic mouse central nervous system. Nature Protocols 1, 1552–1558. doi:10.1038/nprot.2006.276.

Schuch, J. B., Muller, D., Endres, R. G., Bosa, C. A., Longo, D., Schuler-Faccini, L., Ranzan, J., et al (2014). The role of β3 integrin gene variants in Autism Spectrum Disorders--diagnosis and symptomatology. Gene 553(1):24-30. PMID: 25280596.

Scorcioni, R., Polavaram, S., and Ascoli, G. A. (2008). L-Measure: a web-accessible tool for the analysis, comparison and search of digital reconstructions of neuronal morphologies. Nature Protocols 3, 866–876. doi:10.1038/nprot.2008.51.

Shen, Q., Wang, Y., Dimos, J. T., Fasano, C. A., Phoenix, T. N., Lemischka, I. R., *et al.* (2006). The timing of cortical neurogenesis is encoded within lineages of individual progenitor cells. Nature Neuroscience 9, 743–751. doi:10.1038/nn1694.

Shi, Y. and Ethell, I. M. (2006). Integrins control dendritic spine plasticity in hippocampal neurons through NMDA receptor and $Ca^{2+}$/calmodulin-dependent protein kinase II-mediated actin reorganization. J Neurosci. 26(6), 1813-1822.

Sholl, D. A. (1953). Dendritic organization in the neurons of the visual and motor cortices of the cat. J Anat 87(4):387-406. PMCID: PMC1244622.

Singh, A. S., Chandra, R., Guhathakurta, S., Sinha, S., Chatterjee, A., Ahmed, S., Ghosh, S., and Rajamma, U. (2013). Genetic association and gene-gene interaction analyses suggest likely involvement of ITGB3 and TPH2 with autism spectrum disorder (ASD) in the Indian population. Prog Neuropsychopharmacol Biol Psychiatry 45:131-43. PMID: 23628433.

Stancik, E. K., Navarro-Quiroga, I., Sellke, R., and Haydar, T. F. (2010). Heterogeneity in Ventricular Zone Neural Precursors Contributes to Neuronal Fate Diversity in the Postnatal Neocortex. Journal of Neuroscience 30, 7028–7036. doi:10.1523/jneurosci.6131-09.2010.

Tang, G., Gudsnuk, K., Kuo, S. H., Cotrina, M. L., Rosoklija, G., Sosunov, A., *et al*. (2014). Loss of mTOR-dependent macroautophagy causes autistic-like synaptic pruning deficits. Neuron 83(5):1131-43.

Thompson-Peer, K. L., DeVault, L., Li, T., Jan, L. Y., and Jan, Y. N. (2016). In vivo dendrite regeneration after injury is different from dendrite development. Genes & Development 30, 1776–1789. doi:10.1101/gad.282848.116.

Vidal, C. N., Nicolson, R., DeVito, T. J., Hayashi, K. M., Geaga, J. A., Drost, D. J.,
  Williamson, P.C., et al (2006). Mapping corpus callosum deficits in autism: an
  index of aberrant cortical connectivity. Biol Psychiatry 60(3):218-25. PMID:
  16460701.

Vidal, G. S., Djurisic, M., Brown, K., Sapp, R. W., and Shatz, C. J. (2016) Cell-
  Autonomous Regulation of Dendritic Spine Density by PirB. eNeuro 3(5).

Warren, M. S., Bradley, W. D., Gourley, S. L., Lin, Y. C., Simpson, M. A., Reichardt,
  L. F., Greer, C. A., Taylor, J. R., and Koleske, A. J. (2012). Integrin β1 signals
  through Arg to regulate postnatal dendritic arborization, synapse density,
  and behavior. J Neurosci 32(8):2824-34. PMCID: PMC3313657.

Weiss, L. A., Kosova, G., Delahanty, R. J., Jiang, L., Cook, E. H., Ober, C., and
  Sutcliffe, J. S. (2006). Variation in ITGB3 is associated with whole-blood
  serotonin level and autism susceptibility. Eur J Hum Genet 14(8):923-31.
  PMID: 16724005.

Wong, R. O. L., and Ghosh, A. (2002). Activity-dependent regulation of dendritic
  growth and patterning. Nature Reviews Neuroscience 3, 803–812.
  doi:10.1038/nrn941.